Non-Contrast-Enhanced Functional Lung MRI to Evaluate Treatment Response of Allergic Bronchopulmonary Aspergillosis in Patients With Cystic Fibrosis: A Pilot Study

Ilyes Benlala, Rabea Klaar, Thomas Gaass, Julie Macey, Stéphanie Bui, Baudouin Denis de Senneville, Patrick Berger, François Laurent, Gael Dournes, Julien Dinkel

Non-Contrast-Enhanced Functional Lung MRI to Evaluate Treatment Response of Allergic Bronchopulmonary Aspergillosis in Patients With Cystic Fibrosis: A Pilot Study

Ilyes Benlala, Rabea Klaar, Thomas Gaass, Julie Macey, Stéphanie Bui, Baudouin Denis de Senneville, Patrick Berger, François Laurent, Gael Dournes, Julien Dinkel

Abstract

Background: Allergic bronchopulmonary aspergillosis (ABPA) in cystic fibrosis (CF) patients is associated with severe lung damage and requires specific therapeutic management. Repeated imaging is recommended to both diagnose and follow-up the response to treatment of ABPA in CF.

Purpose: To evaluate whether Fourier decomposition (FD) functional lung MRI can detect the response to treatment of ABPA in CF patients.

Study type: Retrospective longitudinal.

Population: 12 patients (7 M, median age: 14 years) with CF and ABPA (according to Cystic Fibrosis Foundation Consensus Conference criteria) and pre- and post-treatment MRI.

Field strength/sequence: 2D balanced steady-state free precession (bSSFP) sequence with Fourier decomposition (FD) at 1.5T.

Assessment: Ventilation weighted (V) and perfusion weighted (Q) maps were obtained after FD processing of 2D coronal bSSFP time resolved images acquired before and 3 – 9 months after treatment of ABPA. Defects extent was assessed on the functional maps using a qualitative semi-quantitative score. Mean and coefficient of variation (cv) of the ventilation signal intensity (VSI) and the perfusion signal intensity (QSI) were calculated. Measurements were performed independently by two readers and averaged. The inter-reader reproducibility of the measurements was also assessed. Pulmonary function tests (PFTs) using body plethysmography were performed within 1 week of both MRI studies as markers of the airflow limitation severity.

Statistical tests: Comparisons of medians were performed using the paired Wilcoxon test. Reproducibility was assessed using the intraclass correlation coefficient (ICC). Correlations between MRI and PFT parameters were assessed using the Spearman test (correlation coefficient: rho). A p value <0.05 was considered as significant.

Results: Defects extent on both V and Q maps showed a significant reduction after ABPA treatment. VSI_mean was significantly increased after treatment. Qualitative analyses reproducibility showed an ICC >0.93, while the ICCs of the quantitative measurements was almost perfect (>0.99). Changes in VSI_cv and QSI_cv before and after treatment correlated inversely with changes of obstructive parameters assessed by PFTs (rho = -0.68 for both).

Data conclusion: Non-contrast enhanced FD lung MRI has potential to reproducibly assess response to treatment of ABPA in CF patients and correlates with PFT obstructive parameters.

Keywords: ABPA; CF; ventilation; perfusion; Fourier decomposition

Introduction

Cystic fibrosis (CF) is one of the most frequent genetic disorders in the Caucasian population [1]. It is caused by mutations in the cystic fibrosis transmembrane conductance regulator (CFTR) gene, resulting in diverse pathologic manifestations including bronchiectasis, nasal polyposis, pancreatic insufficiency, and infertility [2]. Lung involvement (*i.e.*, destruction of lung parenchyma and decline in pulmonary function) is responsible for most life-limiting complications [1]. Mucus composition and thickness in CF patients provide a favourable environment for fungal respiratory infections [3]. Indeed, *Aspergillus fumigatus* has been found in the sputum of up to 57% of patients with CF [4]. The growth of *A. fumigatus* hyphae within the bronchial lumen may be responsible for an immunoglobulin E (IgE)-mediated hypersensitivity response, known as allergic bronchopulmonary aspergillosis (ABPA), leading to bronchial inflammation and airway destruction. Its prevalence in CF patients ranges between 3 to 25%, and is higher than that in asthmatic patients [5]. In CF patients, ABPA, which is associated with severe lung damage and requires specific therapeutic management, may be suspected due to worsening of pulmonary function and evidence of new infiltrates on chest radiographs or computed tomography (CT). Also, the findings of ABPA on chest CT include central bronchiectasis, often with mucoid impaction, centrilobular nodules, mosaic attenuation, and cavitation [6–8]. Another finding of ABPA is high-attenuation mucus plugging (HAM) on CT images, which has been considered highly specific, if not pathognomonic of the disease [9]. One of the important aspects in the management of ABPA in CF patients is repeating imaging after treatment to evaluate the effectiveness of the chosen therapeutics. However, repeating CT examinations should be limited due to the risk associated with high cumulative radiation exposure [10, 11]. Recently, lung MRI has been evaluated to assess structural alterations in CF [12, 13]. Indeed, lung morphological modifications in CF assessed using ultra-short echo time (UTE)-MRI have been found to be similar to those using CT [12, 14]. Furthermore, inverted mucus impaction signal on MRI (IMIS), which is characterized by a high signal intensity on T1-weighted images and low signal intensity on T2-weighted images, can be considered as the counterpart of HAM and has been found to be 100% specific to detect ABPA in CF patients [15]. Moreover, lung MRI can evaluate pulmonary functional changes in a regional fashion [16]. Non-contrast techniques of pulmonary ventilation-perfusion assessment in CF patients (*e.g.*, Fourier decomposition (FD) MRI) have been reported [17, 18]. These have been validated against photon emission computed tomography (SPECT), dynamic contrast-enhanced MRI and hyperpolarized 3He,

which is considered to be the reference standard in assessing lung function using imaging [19]. Nonetheless, longitudinal evaluations before and after treatment of ABPA in CF patients using morphological and functional lung MRI are lacking. We hypothesised that FD-MRI could detect response to treatment in CF patients with ABPA.

Thus, the main aim of this study was to evaluate the response to treatment of ABPA in CF patients based on FD-MRI functional changes. Our secondary aims were to: (a) evaluate morphological changes before and after treatment of ABPA using UTE-MRI; (b) investigate correlations between both morphological and functional alterations and pulmonary function test (PFT) parameters; and (c) assess the structure-function relationships in CF patients with ABPA.

Material and methods

Study population:

This retrospective longitudinal pilot study was performed in a single center and approved by the local ethics committee. The requirement for written consent was waived. All consecutive CF patients referred to our institution, a tertiary CF center, were screened between August 2018 and September 2021. Inclusion criteria were: (a) diagnosis of CF proven by sweat chloride and/or genetic testing, (b) age older than 6 years, (c) diagnosis of ABPA established by multidisciplinary sessions involving pediatricians, pneumologists, physicians, immunologists, physiologists, and mycologists with full knowledge of the patient's medical history and according to the CFFC criteria [20]. All included patients underwent lung MRI with UTE and FD sequences before and after treatment of ABPA. Median interval between the two examinations was 5 months (minimum of 3 months and maximum of 9 months). In addition, total IgE and anti–*A fumigatus* specific IgE levels were measured before and after treatment as well as pulmonary function tests within one week from the lung MRI examinations. Clinical and radiological improvement and/or a drop of at least 25% of total IgE were considered as positive response to ABPA treatments [21].

Pulmonary Function Tests:

PFTs were assessed using body plethysmography (BodyBox, Medisoft. Leeds, UK). Reference values were based on American Thoracic Society and European Respiratory Society guidelines [22, 23]. Measurements of forced expiratory volume in 1 second (FEV1), forced volume capacity (FVC), FEV1/FVC and forced expiratory flow at 25%-75% (FEF_{25-75})

were measured and expressed as percentage of predicted values (FEV1%p, FVC%p, FEV1%p/FVC%p and FEF_{25-75}%p, respectively).

MRI examinations:

MRI examinations were completed on a 1.5 Tesla Siemens Aera scanner (Siemens, Erlangen, Germany). Images of a stack of spirals spoiled ultra-short gradient echo sequence (3D-UTE) were acquired in the supine position using the following parameters: TR/TE/flip angle=4.3ms/0.05ms/5° and a voxel size of $1mm^3$. Respiratory synchronization at end normal expiration was allowed by automated self-navigated respiratory gating. Scan duration was between 6 and 8 minutes. Time resolved images of a 2D balanced steady-state free precession (bSSFP) sequence were acquired in two coronal planes: at the level of the carina and posteriorly at the level of the descending aorta. The main pulse sequence parameters were: TR/TE/flip angle=1.74ms/0.71ms/47°, pixel size of $(1.2x1.2\ mm)^2$ and slice thickness = 12 mm. Each bSSFP series consisted of 200 images. Scan duration was around 1 minute per slice. In addition, for IMIS identification, a T2-weighted radial fast spin-echo (RFSE) sequence was acquired using the following parameters: TR/TEs/flip angle=2350ms/20ms-150ms/145°; pixel size of (1.6 x 1.6) mm^2 and slice thickness = 1.6mm. A T1-weighted VIBE sequence was also acquired using the following parameters: TR/TE/flip angle=3.37ms/1.28ms/8°; pixel size of (1.2 x 1.2) mm^2 and slice thickness = 3mm.

Fourier decomposition (FD) image Processing Workflow:

The image processing workflow was fully implemented in Python (version 3.9). After discarding the first 20 bSSFP images, where the steady state condition was not fulfilled [17], the acquired image series was first elastically registered to a reference image in mid-position between full inspiration and full expiration which was determined automatically using average lung signal variation. The deformable registration was performed using the EVolution algorithm [24], which is based on a similarity term that favours edge alignment and on a diffeomorphic transformation that ensures the preservation of the image topology. Based on this reference image, a manual segmentation of the lung was performed and a region of interest (ROI) drawn within the aorta by two radiologists. The sampling times were used to calculate the fast Fourier Transform (FFT) per pixel in the segmented lung. Ventilation weighted (V) and perfusion weighted (Q) maps were then generated by taking the maximum magnitude of the corresponding peak in the Fourier spectrum using the lung ROI for ventilation and the aorta ROI for perfusion.

Finally, the signal within the V-map and the Q-map was normalized using the mean signal in the aorta ROI of the reference image for each examination.

A muscular ROI was also drawn on the reference image of each examination to check if the overall signal varied between the two examinations before and after treatment.

Functional analysis:

Qualitative evaluation: Defect extents on V and Q maps were assessed using a semi quantitative score (0= absence/negligible, 1=<50%, 2=>50%) regarding the right/left lungs, superior, median or inferior regions for each slice. The score was then averaged between the two acquired slices and ranged between 0 and 12.

Quantitative evaluation: Mean and coefficient of variation (cv) of the signal intensity (SI) of both ventilation and perfusion maps were calculated (*i.e.*, VSI_mean, VSI_cv, QSI_mean and QSI_cv).

Morphological analysis:

A widely used structural alterations scoring system in CF patients (Bhalla score) was implemented [25]. Detection of IMIS was also part of the evaluation [15].

Two radiologists with 5 and 10 years experience in thoracic imaging performed morphological and functional evaluations. All the measurements performed in this study were averaged between the two readers.

Structure-function evaluation:

For the structure-function relationships evaluation, a matched 3D UTE-MRI coronal slice was assessed in terms of structural changes (*i.e.*, bronchiectasis without mucus plugging, bronchiectasis filled with mucus plugging and consolidation) alongside the V and Q maps. Regions were then classified as defect regions or no defect regions and the predominant structural alteration identified. A consensus reading was carried out for these evaluations and scrolling through the adjacent slices of the 3D UTE images was allowed for identification of structural changes.

Statistical analysis:

Statistical analyses were performed using MedCalc software (Version 20.216). Distribution normality was assessed using the Shapiro-wilk test. Data were expressed as medians with

[minimum to maximum range] for continuous variables and absolute numbers for categorical variables. Comparisons of paired medians were performed using the Wilcoxon signed-rank test and paired percentages using the McNemar test; correlations were assessed using the Spearman test (correlation coefficient, rho). A p-value<0.05 was considered statistically significant. Reproducibility was assessed using intraclass correlation coefficients (ICCs), with mixed model analysis and absolute agreement option. ICC values were classified as null (=0), slight (>0 and <0.20), fair (≥0.20 and <0.40), moderate (≥0.40 and <0.60), good (≥0.60 and <0.80), very good (≥0.80 and <0.95) and almost perfect (≥0.95) [26]. Structure-function relationships were evaluated using Chi2 tests.

Results:

Study population

Among 109 CF patients referred to our institution between 2018 and 2021, 29 patients showed an exacerbation attributed to ABPA according to the multidisciplinary care meeting and CFFC criteria. Seventeen patients were not included (nine did not undergo lung MRI before treatment and eight did not have lung MRI after treatment within a maximum interval of one week from the IgE measurements). Twelve patients were therefore included in this study, each having had lung MRI, total IgE and specific IgE measurements and PFTs before and after treatment of ABPA (Figure 1). All included patients showed a positive response to specific treatment (*i.e.*, oral corticosteroids and itraconazole) either with a drop of total IgE or clinical and radiological improvement or both. Patients' characteristics are summarized in Table 1. Median age of the included patients before treatment was 14 years with 7 males and 5 females. The medians of total IgE and specific IgE before treatment were 667.5 UI/ml and 10.5 UI/ml respectively with a significant reduction to 467.5 UI/ml and 8.36 UI/ml respectively after treatment. FEV1%p showed a significant improvement after ABPA treatment with the median FEV1%p increasing from 61% to 67%.

Comparison of functional FD-MRI ventilation and perfusion before and after ABPA treatment

The extent of the ventilation and perfusion defects decreased significantly after ABPA treatment reflecting a significant improvement of the lung function evaluated using FD-MRI (Table 2, Figure 2 and Figure 3).

Using the fully automated quantification of lung ventilation, the median of VSI_mean was significantly increased after ABPA treatment (Table 2, Figure 3) reflecting a global

improvement of the lung ventilation whereas QSI_mean showed only a non-significant trend for increase after treatment (Table 2, Figure 3). Regarding the heterogeneity of V map and Q map, the VSI_cv and QSI_cv did not demonstrate significant changes after ABPA treatment (p=0.33 and p=0.62, respectively) (Table 2).

No statistically significant difference was found between the mean and the standard deviation of the signal in the muscular ROIs before and after treatment (p=0.42) (Table E1).

Comparison of morphological Bhalla score before and after ABPA treatment

The median of the MR-Bhalla score was significantly increased after ABPA treatment reflecting a decrease of structural alterations' severity assessed using 3D UTE morphological MRI. In addition, 6 patients showed an IMIS on lung MRI before treatment which were not present on the follow-up MRI (p=0.03) (Table 2).

Correlations with the pulmonary function tests

Before treatment, no significant correlation was found between PFT parameters and lung MRI functional or morphological measurements. After treatment, ventilation defects extent assessed visually was inversely correlated to PFT obstructive parameters (Table E2). Using quantitative imaging, QSI_mean was significantly correlated to FEV1%p and QSI_cv showed a significant inverse correlation with FEF25-75%p (Table E2). The MR-Bhalla score also showed a significant correlation with PFTs' obstructive parameters after treatment (Table E2).

However, only changes in quantitative functional imaging parameters before and after treatment (*i.e.,* ΔVSI_cv and ΔQSI_cv) showed significant correlations with changes of PFT obstructive parameters before and after treatment (ΔFEV1%p and ΔFEF25-75%p) (Figure 4, Table E3).

Assessment of reproducibility

Very good inter-observer reproducibility was obtained for functional and morphological qualitative scores (ICC>0.93). Reproducibility of quantitative measurements was almost perfect, with ICCs >0.99 (Table 3).

Structure-function relationships

A total of 576 regions were evaluated. Three hundred and twenty-two (322) regions had no defect and 254 had defects (130 with Q defects and 124 with V defects). Regarding the defect extent, there were115 defects with less than 50% extent and 139 with more than 50% extent.

According to structural alterations evaluated in this study (Table 4), the presence of bronchiectasis without mucus plugging was found in 13 regions without any defects, and no bronchiectasis without mucus plugging was found in regions with V or Q defects. Bronchiectasis with mucus plugging was found in 39 regions without any defect and in 232 regions with V or Q defects (Figure 5). Consolidations were found only in regions with V or Q defects (18 regions). Only 4 regions showed functional defects (1 with V defects and 3 with Q defects) without any visible structural alteration. Presence of structural alterations was not different between regions with V defects and regions with Q defects (p=0.06). The presence of functional defects (V or Q) was significantly different between regions with structural alterations and regions with no visible structural alterations. In addition, the presence of functional defects (V or Q) differed significantly according to the structural alterations assessed. Only 6 regions showed a mismatch between V and Q defects (p=0.33).

Moreover, no correlations were found between the MR-Bhalla morphological score and both qualitative and quantitative evaluations of ventilation and perfusion (p>0.30) (Table E4).

Discussion:

We demonstrated in this study that lung functional FD-MRI is able to assess ventilation and perfusion defects in CF patients with ABPA. We also showed that automatic quantification of lung V and Q is feasible in CF patients with ABPA using FD-MRI. Our findings showed that the extent of V and Q defects decreased after positive response to treatment of ABPA in CF patients. Moreover, we found an increase of VSI_mean after treatment. Our qualitative and automatic quantitative methods showed a very good to almost perfect inter-reader reproducibility. Interestingly, only the pre and post-ABPA treatment changes in VSI_cv and QSI_cv, reflecting more homogenous V and Q maps following treatment, were found to correlate with pre- and post-ABPA treatment changes of FEV1%p. Finally, we showed that functional defects are associated with structural alterations, especially with mucus plugging and consolidations.

Regarding morphological lung MRI, our findings are in line with previously reported results which showed a complete resolution of IMIS in the follow-up [15]. Moreover, a recent study [27] has shown that free breathing phase resolved functional lung MRI imaging could detect improvement following exacerbation treatments using antibiotics out of the context of ABPA. Furthermore, recent studies have demonstrated the benefit of using other MRI techniques (*i.e.*,

diffusion weighted imaging and T2 weighted imaging) in monitoring CF exacerbations [28, 29].

In this study, functional defects were found to be associated with ABPA exacerbation and showed a significant decrease after specific treatment. Indeed, CF patients with ABPA are prone to more severe exacerbations and require a specific treatment and repeated imaging. However, iterative radiation exposure raises concerns in young CF patients with a need of a radiation-free alternative. Moreover, FD-MRI is performed without any contrast agent administration, and thus avoids long-term effects of MRI contrast deposition [30].

In this study, automatic quantification of VSI and QSI also showed an improvement inof global respiratory function after specific ABPA treatment. We used a simple normalization technique to account for signal intensity bias in longitudinal examinations and we also confirmed that the signal in a muscular ROI was not different between the pre- and post-treatment examinations. Interestingly, the pre- and post-treatment changes of VSI_cv and QSI_cv, which represent the homogeneity of V and Q maps, were correlated to the pre- and post-treatment change of FEV1%p. Thus, the decrease in the number and the extent of functional defects was associated with more homogenous maps and improved PFTs obstructive parameters. Insights into local and regional respiratory function allowed by the FD-MRI has potential to bring complementary information to the global evaluation of the respiratory function using PFTs in addition to the morphological information available from 3D UTE-MRI.

Morphological MR-Bhalla score was also found improved in the follow-up, which is in line with previously published data on structural changes in the follow-up of exacerbations in CF patients [31–34].

In our study, we found that functional defects were associated with structural lung alterations without any distinction between V defects and Q defects. However, bronchiectasis without mucus plugging was not associated with functional defects assessed by using FD-MRI. Indeed, airway obstruction is more likely responsible for matched ventilation-perfusion defects. However, since we did not assess the relationship between the severity of the bronchiectasis and functional defects, our findings need to be interpreted with caution.

Limitations

First, this was a retrospective pilot study in a small number of patients. However, the patients included had a high confidence diagnosis of ABPA and also had IgE serological measurements performed before and after treatment close to the MRI examinations. However, large prospective cohorts to validate our findings are needed. Second, in this study, we did not correlate FD-MRI findings to dynamic contrast enhanced (DCE) MRI or to hyperpolarized gas MRI. However, functional FD-MRI has already been validated using these techniques [19, 35]. Third, although our qualitative evaluation of functional defects showed a high inter-reader reproducibility, it could be worth using an automatic relative quantification of defects based on threshold techniques [36]. Finally, a further comparison of different non-rigid image registration algorithms may provide information about the robustness of these findings regarding preprocessing techniques.

Conclusion

Functional changes in CF patients with ABPA may be reproducibly assessed using FD lung MRI and correlate with pulmonary function test changes after specific treatment of ABPA. Therefore, non-contrast enhanced functional FD lung MRI has potential be used to monitor treatment of ABPA in CF patients.

References

1. Jain M, Goss CH (2014) Update in Cystic Fibrosis 2013. Am J Respir Crit Care Med 189:1181–1186. https://doi.org/10.1164/rccm.201402-0203UP

2. Sheppard MN, Nicholson AG (2002) The pathology of cystic fibrosis. Curr Diagn Pathol 8:50–59. https://doi.org/10.1054/cdip.2001.0088

3. Kousha M, Tadi R, Soubani AO (2011) Pulmonary aspergillosis: a clinical review. Eur Respir Rev 20:156–174. https://doi.org/10.1183/09059180.00001011

4. Saunders RV, Modha DE, Claydon A, Gaillard EA (2016) Chronic Aspergillus fumigatus colonization of the pediatric cystic fibrosis airway is common and may be associated with a more rapid decline in lung function. Med Mycol 54:537–543. https://doi.org/10.1093/mmy/myv119

5. Mastella G, Rainisio M, Harms HK, et al (2000) Allergic bronchopulmonary aspergillosis in cystic fibrosis. A European epidemiological study. Epidemiologic Registry of Cystic Fibrosis. Eur Respir J 16:464–471. https://doi.org/10.1034/j.1399-3003.2000.016003464.x

6. Ward S, Heyneman L, Lee MJ, et al (1999) Accuracy of CT in the diagnosis of allergic bronchopulmonary aspergillosis in asthmatic patients. AJR Am J Roentgenol 173:937–942. https://doi.org/10.2214/ajr.173.4.10511153

7. Neeld DA, Goodman LR, Gurney JW, et al (1990) Computerized tomography in the evaluation of allergic bronchopulmonary aspergillosis. Am Rev Respir Dis 142:1200–1205. https://doi.org/10.1164/ajrccm/142.5.1200

8. Logan PM, Müller NL (1996) High-attenuation mucous plugging in allergic bronchopulmonary aspergillosis. Can Assoc Radiol J J Assoc Can Radiol 47:374–377

9. Refait J, Macey J, Bui S, et al (2019) CT evaluation of hyperattenuating mucus to diagnose allergic bronchopulmonary aspergillosis in the special condition of cystic fibrosis. J Cyst Fibros Off J Eur Cyst Fibros Soc 18:e31–e36. https://doi.org/10.1016/j.jcf.2019.02.002

10. Brenner DJ, Hall EJ (2007) Computed tomography--an increasing source of radiation exposure. N Engl J Med 357:2277–2284. https://doi.org/10.1056/NEJMra072149

11. Pearce MS, Salotti JA, Little MP, et al (2012) Radiation exposure from CT scans in childhood and subsequent risk of leukaemia and brain tumours: a retrospective cohort study. Lancet Lond Engl 380:499–505. https://doi.org/10.1016/S0140-6736(12)60815-0

12. Dournes G, Menut F, Macey J, et al (2016) Lung morphology assessment of cystic fibrosis using MRI with ultra-short echo time at submillimeter spatial resolution. Eur Radiol 26:3811–3820. https://doi.org/10.1007/s00330-016-4218-5

13. Dournes G, Grodzki D, Macey J, et al (2015) Quiet Submillimeter MR Imaging of the Lung Is Feasible with a PETRA Sequence at 1.5 T. Radiology 276:258–265. https://doi.org/10.1148/radiol.15141655

14. Dournes G, Yazbek J, Benhassen W, et al (2018) 3D ultrashort echo time MRI of the lung using stack-of-spirals and spherical k-Space coverages: Evaluation in healthy volunteers and parenchymal diseases. J Magn Reson Imaging JMRI 48:1489–1497. https://doi.org/10.1002/jmri.26212

15. Dournes G, Berger P, Refait J, et al (2017) Allergic Bronchopulmonary Aspergillosis in Cystic Fibrosis: MR Imaging of Airway Mucus Contrasts as a Tool for Diagnosis. Radiology 285:261–269. https://doi.org/10.1148/radiol.2017162350

16. Dournes G, Walkup LL, Benlala I, et al (2021) The Clinical Use of Lung MRI in Cystic Fibrosis: What, Now, How? CHEST 159:2205–2217. https://doi.org/10.1016/j.chest.2020.12.008

17. Bauman G, Puderbach M, Deimling M, et al (2009) Non-contrast-enhanced perfusion and ventilation assessment of the human lung by means of fourier decomposition in proton MRI. Magn Reson Med 62:656–664. https://doi.org/10.1002/mrm.22031

18. Bondesson D, Schneider MJ, Gaass T, et al (2019) Nonuniform Fourier-decomposition MRI for ventilation- and perfusion-weighted imaging of the lung. Magn Reson Med 82:1312–1321. https://doi.org/10.1002/mrm.27803

19. Bauman G, Scholz A, Rivoire J, et al (2013) Lung ventilation- and perfusion-weighted Fourier decomposition magnetic resonance imaging: in vivo validation with hyperpolarized 3He and dynamic contrast-enhanced MRI. Magn Reson Med 69:229–237. https://doi.org/10.1002/mrm.24236

20. Stevens DA, Moss RB, Kurup VP, et al (2003) Allergic Bronchopulmonary Aspergillosis in Cystic Fibrosis—State of the Art: Cystic Fibrosis Foundation Consensus Conference. Clin Infect Dis 37:S225–S264. https://doi.org/10.1086/376525

21. Agarwal R, Chakrabarti A, Shah A, et al (2013) Allergic bronchopulmonary aspergillosis: review of literature and proposal of new diagnostic and classification criteria. Clin Exp Allergy J Br Soc Allergy Clin Immunol 43:850–873. https://doi.org/10.1111/cea.12141

22. Miller MR, Hankinson J, Brusasco V, et al (2005) Standardisation of spirometry. Eur Respir J 26:319–338. https://doi.org/10.1183/09031936.05.00034805

23. Wanger J, Clausen JL, Coates A, et al (2005) Standardisation of the measurement of lung volumes. Eur Respir J 26:511–522. https://doi.org/10.1183/09031936.05.00035005

24. Denis de Senneville B, Zachiu C, Ries M, Moonen C (2016) EVolution: an edge-based variational method for non-rigid multi-modal image registration. Phys Med Biol 61:7377–7396. https://doi.org/10.1088/0031-9155/61/20/7377

25. Bhalla M, Turcios N, Aponte V, et al (1991) Cystic fibrosis: scoring system with thin-section CT. Radiology 179:783–788. https://doi.org/10.1148/radiology.179.3.2027992

26. Landis JR, Koch GG (1977) The measurement of observer agreement for categorical data. Biometrics 33:159–174

27. Munidasa S, Couch MJ, Rayment JH, et al (2021) Free-breathing MRI for monitoring ventilation changes following antibiotic treatment of pulmonary exacerbations in paediatric cystic fibrosis. Eur Respir J 57:. https://doi.org/10.1183/13993003.03104-2020

28. Ciet P, Bertolo S, Ros M, et al (2017) Detection and monitoring of lung inflammation in cystic fibrosis during respiratory tract exacerbation using diffusion-weighted magnetic resonance imaging. Eur Respir J 50:. https://doi.org/10.1183/13993003.01437-2016

29. Benlala I, Hocke F, Macey J, et al (2019) Quantification of MRI T2-weighted High Signal Volume in Cystic Fibrosis: A Pilot Study. Radiology 190797. https://doi.org/10.1148/radiol.2019190797

30. Rozenfeld MN, Podberesky DJ (2018) Gadolinium-based contrast agents in children. Pediatr Radiol 48:1188–1196. https://doi.org/10.1007/s00247-018-4165-1

31. Shah RM, Sexauer W, Ostrum BJ, et al (1997) High-resolution CT in the acute exacerbation of cystic fibrosis: evaluation of acute findings, reversibility of those findings, and clinical correlation. Am J Roentgenol 169:375–380. https://doi.org/10.2214/ajr.169.2.9242738

32. Davis SD, Fordham LA, Brody AS, et al (2007) Computed tomography reflects lower airway inflammation and tracks changes in early cystic fibrosis. Am J Respir Crit Care Med 175:943–950. https://doi.org/10.1164/rccm.200603-343OC

33. Byrnes CA, Vidmar S, Cheney JL, et al (2013) Prospective evaluation of respiratory exacerbations in children with cystic fibrosis from newborn screening to 5 years of age. Thorax 68:643–651. https://doi.org/10.1136/thoraxjnl-2012-202342

34. Wielpütz MO, Puderbach M, Kopp-Schneider A, et al (2014) Magnetic resonance imaging detects changes in structure and perfusion, and response to therapy in early cystic fibrosis lung disease. Am J Respir Crit Care Med 189:956–965. https://doi.org/10.1164/rccm.201309-1659OC

35. Bauman G, Puderbach M, Heimann T, et al (2013) Validation of Fourier decomposition MRI with dynamic contrast-enhanced MRI using visual and automated scoring of pulmonary perfusion in young cystic fibrosis patients. Eur J Radiol 82:2371–2377. https://doi.org/10.1016/j.ejrad.2013.08.018

36. Nyilas S, Bauman G, Sommer G, et al (2017) Novel magnetic resonance technique for functional imaging of cystic fibrosis lung disease. Eur Respir J 50:1701464. https://doi.org/10.1183/13993003.01464-20

Tables:

Table 1. Clinical and functional characteristics of study participants

		Before Treatment (n=12)	After Treatment (n=12)	p-value
Age	Years	14 [6.5-32]	14 [7-33]	<0.01
Sex ratio	Male/Female	7 / 5	7 / 5	0.77
BMI	$kg.m^{-2}$	18.5 [13-22]	19 [14-23]	0.95
Mutation ΔF508	Homozygous (yes/no)	7 / 5	7 / 5	0.77
Total IgE	UI/ml	667.5 [221-3529]	467.5 [26-1917]	<0.01
Anti–*A fumigatus* Specific IgE	UI/ml	10.5 [2.15-32.3]	8.36 [0-25.3]	<0.01
PFT	FEV_1 (%p)	61 [20-106]	67 [22-126]	<0.01
	FVC (%p)	78 [30-107]	93 [32-131]	<0.01
	FEV_1/FVC	74 [55-100]	71 [51-103]	0.84
	FEF_{25_75} (%p)	28 [8-95]	32.5 [9-104]	0.15

Note: Data are median with [minimum to maximum range] for continuous variables and absolute number for categorical variables. Legends: ABPA= allergic bronchopulmonary aspergillosis; BMI=body mass index; IgE= immunoglobulin E; FEV1=forced expiratory volume in 1 second; FVC=forced volume capacity; FEF25-75=forced expiratory flow at 25%-75%; %p=percentage of predicted value

Table 2. Imaging characteristics of study participants

		Before Treatment (n=12)	After Treatment (n=12)	p-value
Qualitative Analysis				
Functional evaluation	V defect score	4.125 [3-10.75]	2 [1-7.25]	<0.01
	Q defect score	5 [2.5-10.75]	2.75 [0-7]	<0.01
Morphological evaluation	MR-Bhalla score	12.75 [9-21]	15.5 [9.5-21]	0.02
	IMIS (present/absent)	6/ 6	0/ 12	0.03
Quantitative Analysis				
	VSI_mean (au)	167 [100-532]	280 [112-535]	<0.01
	VSI_cv	1.18 [0.96-2.09]	1.16 [0.62-1.76]	0.33
	QSI_mean (au)	112 [53-298]	122 [46-282]	0.85
	QSI_cv	1.32 [0.99-1.97]	1.30 [0.82-1.92]	0.62

Note: Data are median with [minimum to maximum range] for continuous variables and absolute number for categorical variables. Legends: IMIS= inverted mucus signal intensity; V= ventilation; Q= perfusion; VSI= ventilation signal intensity; QSI= perfusion signal intensity; au= arbitrary unit; cv= coefficient of variation

Table 3. Interobserver reproducibility of qualitative and quantitative analyses

N=24			**ICC**	**95% CI**
Qualitative Analysis				
	Morphological evaluation	MR-Bhalla score	0.93	0.76-0.97
	Functional evaluation	V defect score	0.97	0.93-0.98
		Q defect score	0.98	0.95-0.99
Quantitative Analysis				
		VSI_mean	>0.99	0.99-1
		VSI_cv	>0.99	0.99-1
		QSI_mean	>0.99	0.99-1
		QSI_cv	>0.99	0.99-1

Legends: ICC= intraclass correlation coeficient ; CI= confidence interval ; ABPA= allergic bronchopulmonary aspergillosis; V= ventilation; Q= perfusion; VSI= ventilation signal intensity; QSI= perfusion signal intensity; cv= coefficient of variation

Table 4. Structure-function evaluation in 576 lung regions

	No defects	V defects		Q defects	
		<50%	>50%	<50%	>50%
Bronchiectasis without MP	13	0	0	0	0
Bronchiectasis with MP	39	49	65	52	66
Consolidation	0	5	4	5	4
No visible structural alteration	270	1	0	3	0

Data are absolute numbers. Legends: V= ventilation, Q= perfusion, MP= mucus plugging

Figure legends:

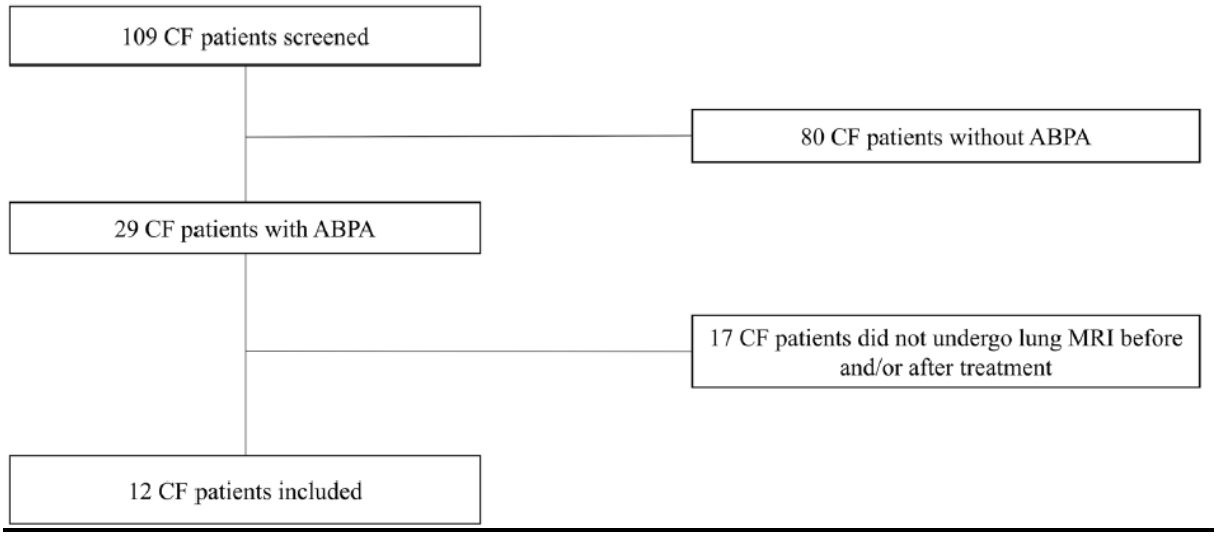

Figure 1: Flowchart of the study. CF= cystic fibrosis; ABPA= allergic bronchopulmonary aspergillosis.

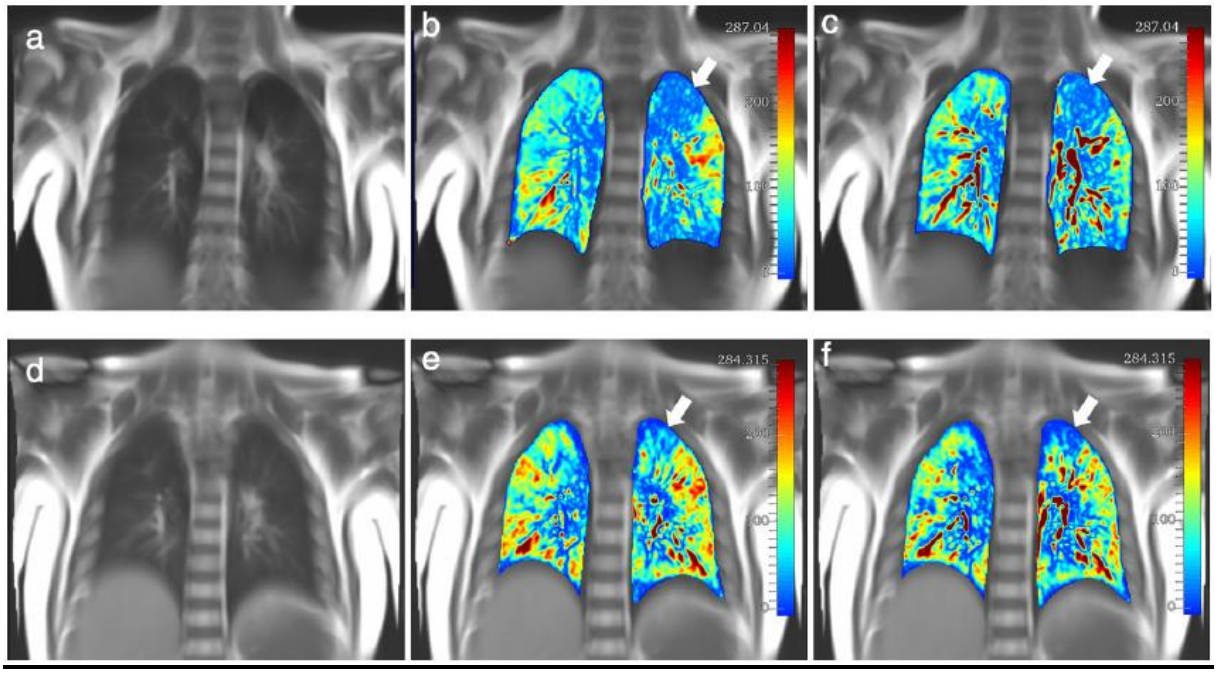

Figure 2: Coronal 2D balanced steady-state free precession image of the lungs of a 16 year old male CF patient before (A) and after (D) ABPA treatment. Note the matched defect of ventilation (B) and perfusion (C) before specific treatment (white arrows) with the decrease in the extent of the defects after treatment on both ventilation map (E) and perfusion map (F).

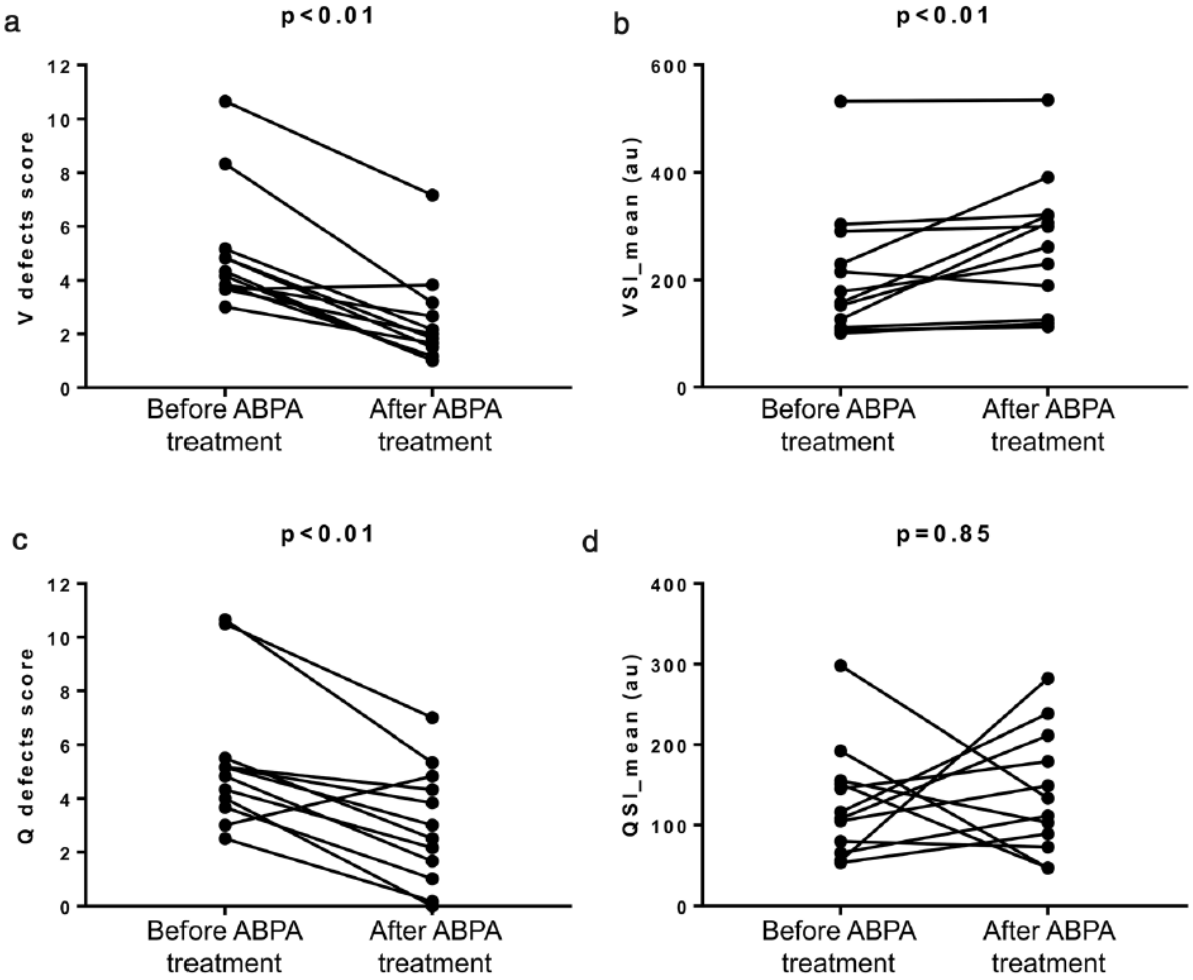

Figure 3: Paired comparisons of the qualitative and quantitative functional FD-lung MRI before and after ABPA treatment. ABPA= allergic bronchopulmonary aspergillosis ; V= ventilation; Q= perfusion; VSI= ventilation signal intensity; QSI= perfusion signal intgensity ; au= arbitrary unit.

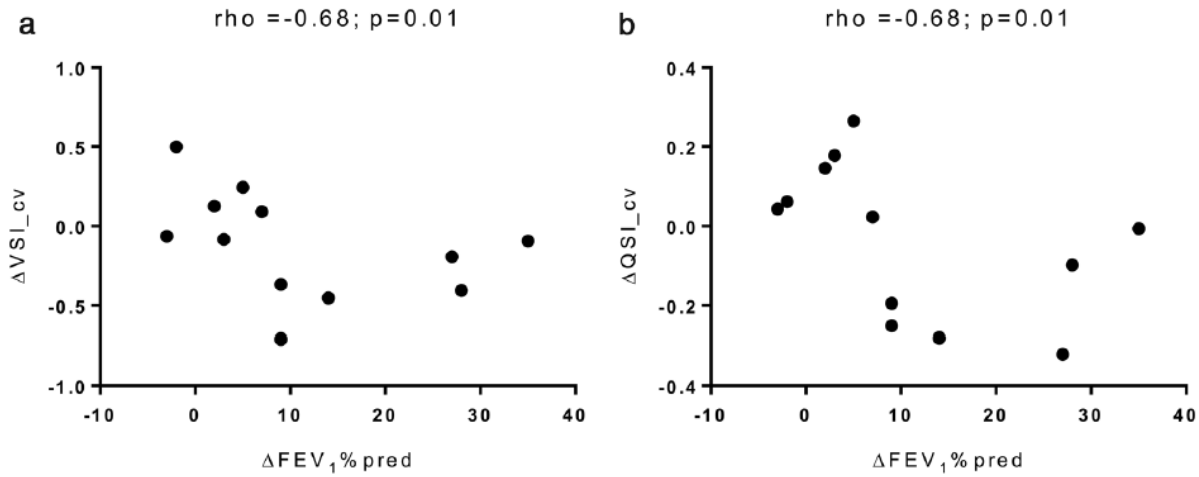

Figure 4: Spearman correlations between the change of FEV1%p and the change of both ventilation and perfusion coefficents of variation before and after treatment (ΔVSI_cv and ΔQSI_cv).

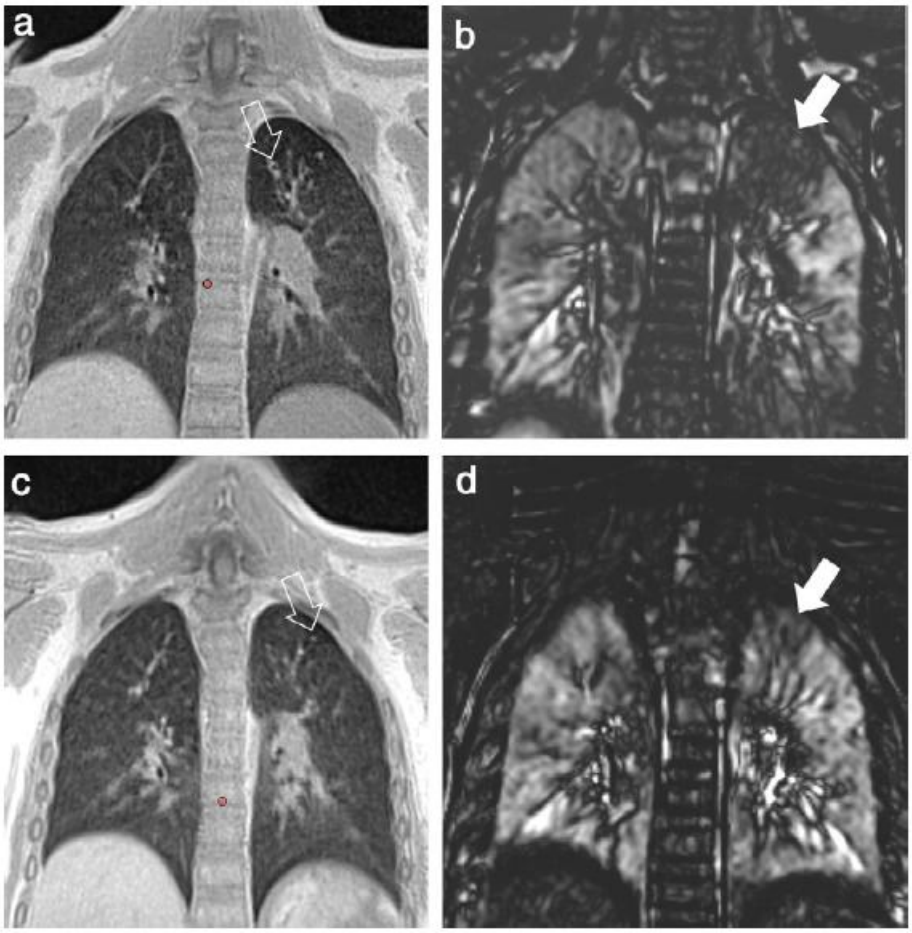

Figure 5: Matched coronal slice of the lung UTE-MRI image and FD ventilation map of a 16 year old male CF patient before (A, B) and after (C, D) ABPA treatment. Note the ventilation defect indicated by the solid arrows before (B) and after (D) treatment and the structural alterations (hollow arrows) seen on the UTE-MRI images showing mucus plugging (A) decreasing after treatment (C).